CHAPTER 4

Evaluation of NPS Return Flow to the River Using a Water Balance Model

4.1. Water Balance Model Applied to the LARV

Water Balance Model Equation.

The purpose of the water balance model is to determine the volume of unaccounted for water in each reach. We begin with a basic water balance model as describe in most hydrology texts — (Wanielista, Kersten, Eaglin, et al. 1997).

change in storage = inputs - outputs

Adding the variables, both known and unknown, present in the LARV we have the following equation:

$$\frac{\Delta S}{\Delta t} = Q_{in,US} + \sum Q_{in} + P + R + B - Q_{out,DS} - \sum Q_{out} - E - T - F \qquad (1)$$

Where:

$\frac{\Delta S}{\Delta t}$ = Stored volume change between time steps.

$Q_{in,US}$ = Flow in the river entering the study reach at the upstream end.

$\sum Q_{in}$ = Flow gained by the river from tributaries and other gauged sources.

P = Volume of water gained to the river due to precipitation falling directly on the river's surface.

R = Volume of water gained to the river due to precipitation runoff from adjacent land.

B = Volume of water gained to the river due to subsurface flow.

$Q_{out,DS}$ = Flow in the river leaving the study reach at the downstream end.

$\sum Q_{out}$ Flow lost from the river to canals and other gauged sinks.

E = Volume of water lost from the river due to direct evaporation from the water's surface.

T = Volume of water lost from the river due to plant transpiration.

F = Volume of water lost from the river due to infiltration into the subsurface flow.

If we combine the terms that are unknown or unmeasured, we arrive at the following equation:

$$\frac{\Delta S}{\Delta t} = Q_{in,US} + \sum Q_{in} + P - Q_{out,DS} - \sum Q_{out} - E + Q_{NPS} \tag{2}$$

Where:

Q_{UNPS}= The sum of gains from non-point sources and losses to non-point sinks ($Q_{NPS} = R + B - T - F + Q_{U,in} - Q_{U,out}$).

There is no reasonable method for differentiating the components of Q_{UNPS}, therefore the abbreviation NPS in this thesis refers to both non-point sources and non-point sinks. Q_{UNPS}includes the non-point source gains from groundwater sources(B), non-point source losses to groundwater sinks F), transpiration losses from plants in the river channel (T), and gains from precipitation runoff from adjacent land (R). Additionally, this term includes ungauged flows leaving and entering the river. Ungauged gains to the river ($Q_{U,in}$) are suspected to be primarily in the form of irrigation drainage from adjacent farmland. Other sources could be due to errors in underestimating flows entering the river or overestimating flows leaving the river. Ungauged losses from the river ($Q_{U,out}$) are suspected to be primarily in the form of minor or unauthorized withdrawals from the river channel. Of the

ungauged flows, irrigation drainage from adjacent farmlands is assumed to be the largest contributor.

The two groundwater components of $Q_{UNPS}$are suspected of being the largest components of Q_{UNPS}. Water transfer between the aquifer and river happens continually whereas $Q_{U,in}$, $Q_{U,out}$, R, and T are not continuous. $Q_{U,in}$ and $Q_{U,out}$ only occur periodically when individuals actively withdraw from the river or allow irrigation runoff to return to the river. R only occurs during rain events. Within the LARV, most rainwater is captured in irrigation canals. Only precipitation falling in the riparian zone is likely to reach the river. T only occurs during growing season. This value is also only considering the transpiration happening within the river channel and does not include the riparian zone. Any losses due to transpiration in the riparian zone are first considered river losses to the aquifer (F).

Re-arranging equation (2) to solve for the unknown values produces equation 3. Due to the nearly identical method of calculating flow (Q) and it's associated error and uncertainty, these terms were associated with each other. Likewise, the precipitation (P) and evaporation (E) terms were associated with each other.

$$Q_{UNPS} = \left(Q_{out,DS} + \sum Q_{out} - Q_{in,US} - \sum Q_{in}\right) - \frac{\Delta S}{\Delta t} - (P + E) \tag{3}$$

A time step of one day was established for all models calculated in this thesis. Most of the data from agencies is readily available in average daily format. While most of the data could also be obtained in hourly or quarter-hourly format, it was assumed that the additional information would not improve model accuracy.

4.2. Stochastic and Deterministic Models

Deterministic and stochastic models are used in both the unaccounted for water and mass balance models. Deterministic models are fully determined by the input parameters or variables. Randomness of any kind is not included. Stochastic models extend deterministic models by including one or more random parameters. Given the same input parameter values, a stochastic model will produce different results with each iteration.

There are many recognized methods for solving stochastic models. Solutions to these models are not definite and the term "solve" must be taken loosely. Any individual solution from a stochastic model is one of a potentially infinite number of possible solutions. The Monte Carlo (MC) simulation technique was used to obtain solutions for all stochastic models in this thesis. The MC technique is conceptually simple. The stochastic model is repetitively solved in a series of iterations. The combined solutions from all iterations are used to define the solution statistics of the model.

The number of iterations performed is determined by calculating and analyzing a set of identifier statistic(s) after each run. Identifier statistic(s) are those that the modeler has determined to be of value in determining when to terminate the model. These statistics are monitored to identify when the change in the statistic has reached a predetermined threshold. It was determined that for the sake of simplicity, all of the models calculated in this thesis would use the same number of iterations. The USR mass balance model is the most complex model as it has the largest number of input variables and uncertainty terms. The identifier statistics used were the mean, variance, and skewness which are the first, second, and third moments of the probability density. These were calculated for each iteration. The threshold between the observed iteration and the previous iteration was fixed at 0.1%. The identifier statistics reached the threshold in the following order: mean, variance, and

skewness. Skewness reached its break point shortly before the 500th iteration. A judgment call was made to increase the factor of safety. Therefore, the number of stochastic model iterations was fixed at 5,000. The fourth moment, kurtosis, was also calculated and analyzed for each iteration. It was found to be too sensitive as it did not consistently stay within the accepted cutoff threshold of 0.1%. It is assumed that this sensitivity is due to the existence of a significant number of outliers that cause the distribution of results to be non-normal.

4.3. Error and Uncertainty.

Any problem that measures variable natural processes must account for parameter and model uncertainties (Vicens, Rodríguez-Iturbe, and Schaake 1975). Parameter uncertainty is derived from measurement error, spatial variability, and temporal variability (Herschy 2002). Measurement error is the difference between the true and measured values. Most of this error type is due to instrument measurement inaccuracies due to either error inherent in the instrument or from errors in calibration or measurement. Measurement errors inherent to the instrument are uncorrectable and cannot be accounted for within the model. Errors due to calibration or measurement deviations are only correctable at the time of measurement or calibration and cannot be accounted for within the model.

Spatial variability is the difference in the true value at different points when measured at the same time. Data collected at a single given point in space may not be representative of the area it is assumed to represent due to spatial variability. This can manifest itself even with very small distances between measurements. Temporal variability is the difference in the true value at the same point, but at different times. Data collected at a one time may not be representative of the time frame it is assumed to represent due to temporal variability (Gates and Al-Zahrani 1996). Again, this can be manifested even over small time differences. Due

to instrument error, the spatiotemporal variability of the measured object, and the inability to know the true value of the measurement, reported parameter values should be treated as random variables (C. T. Haan 1989; Charles Thomas Haan 2002).

Almost all of the data was obtained from outside agencies and was not collected by the research team. These agencies have data uncertainty ranges that account for all parameter uncertainties. These uncertainties are expressed in accordance with the ISO Guide to Expression of Uncertainty in Measurement (GUM) (ISO 2008). While the GUM classifies uncertainty as either "Type A" or "Type B", the all of the data included in this thesis has uncertainty evaluations described as "Type B". Type B evaluations usually use standard deviations and assumed probability distributions obtained from scientific judgment, available information, and possible variability of a measurement.

The data originators have provided uncertainty ranges which include instrument measurement random error and uncertainties due to temporal variations of the measured location. The root mean square method is used to estimate the uncertainty related to measurement of water quantity and water quality values (Harmel and Smith 2007; ISO 2008). Harmel and Smith (2007) describe this measurement uncertainty as the probably error range, and quantify upper and lower uncertainty boundaries for measured data points as the following when attempting to specify an expected range of expected values.

$$\sigma^2 = \left(\frac{O_i - UO_i(l)}{3.9}\right)^2 \qquad or \qquad \sigma^2 = \left(\frac{UO_i(u) - O_i}{3.9}\right)^2 \tag{4}$$

Where:

$\sigma^2 =$ variance about measured data value O_i.

$O_i =$ measured value.

$UO_i =$ upper (u) and lower (l) uncertainty boundaries.

$3.9 =$ number of standard deviations accounting for $> 99.99\%$ of a normal probability distribution

The data collected for this thesis is assumed to represent the mean of a normal distribution of possible values. The upper and lower bounds of the distributions are given as either a percent or value deviation from the mean. Equation 4 is re-written from the definition found in Harmel and Smith (2007) to that found in equation 5.

$$\sigma^2 = \left(\frac{\mu - (\mu - \mu p)}{3.9}\right)^2 \qquad or \qquad \sigma^2 = \left(\frac{(\mu + \mu p) - \mu}{3.9}\right)^2 \tag{5}$$

Where:

$\mu =$ the reported value (assumed to be the mean).

$p =$ the reported percent deviation from μ.

Both of these equations in 5 simplify to equation 6. The standard deviation is shown as the calculated result due to the requirements of the modeling software.

$$\sigma = \frac{\mu p}{3.9} \tag{6}$$

When the upper and lower bounds are defined as a fixed value deviation from the reported value, then equation 4 becomes:

$$\sigma^2 = \left(\frac{\mu - (\mu - v)}{3.9}\right)^2 \qquad or \qquad \sigma^2 = \left(\frac{(\mu + v) - \mu}{3.9}\right)^2 \tag{7}$$

Where:

$v =$ the reported value deviation from μ.

In this case, both equations in 7 simplify to:

$$\sigma = \frac{v}{3.9} \tag{8}$$

The difference between a model's calculated or estimated value and the reported value is called a residual. The distribution of residuals is the model uncertainty. These distributions are uni-variate and do not have predefined shapes. There are a variety of statistical and graphical tools available to analyze unknown residual distributions to determine a best fit parametric distribution. The two graphical tools used in this thesis to analyze distributions are the histogram and the kernel density estimate.

Non-parametric distribution models are used as an aid for analyzing uni-variate data sets. Specifically, kernel density estimates (KDE) are used in conjunction with histograms to assist in visual analysis of the data. Figure 4.1 is an example of a random sample of one of the input data sets used in this thesis. The curve is the KDE. The short vertical lines between the histogram and the x-axis, called a rug, depict the data values. This figure adequately displays the resulting differences between histograms and KDE. KDEs can more accurately depict data groupings that are lost in histogram bins. The histogram leads us to believe that the data has a strong tendency to be near zero, wile the KDE shows that the majority of the data is between 0-20. Histograms can more accurately depict extremes

or cut-off values. In the figure, there are no values less than zero. The histogram clearly shows this while the KDE shows that there are values less than zero. Both histograms and KDE are used throughout this thesis to assist in the description of distributions. A rug is also presented with the histogram whenever the quantity of data allows for adequate data presentation. A rug is not included when the data set is too large to allow for discreet identification of data values.

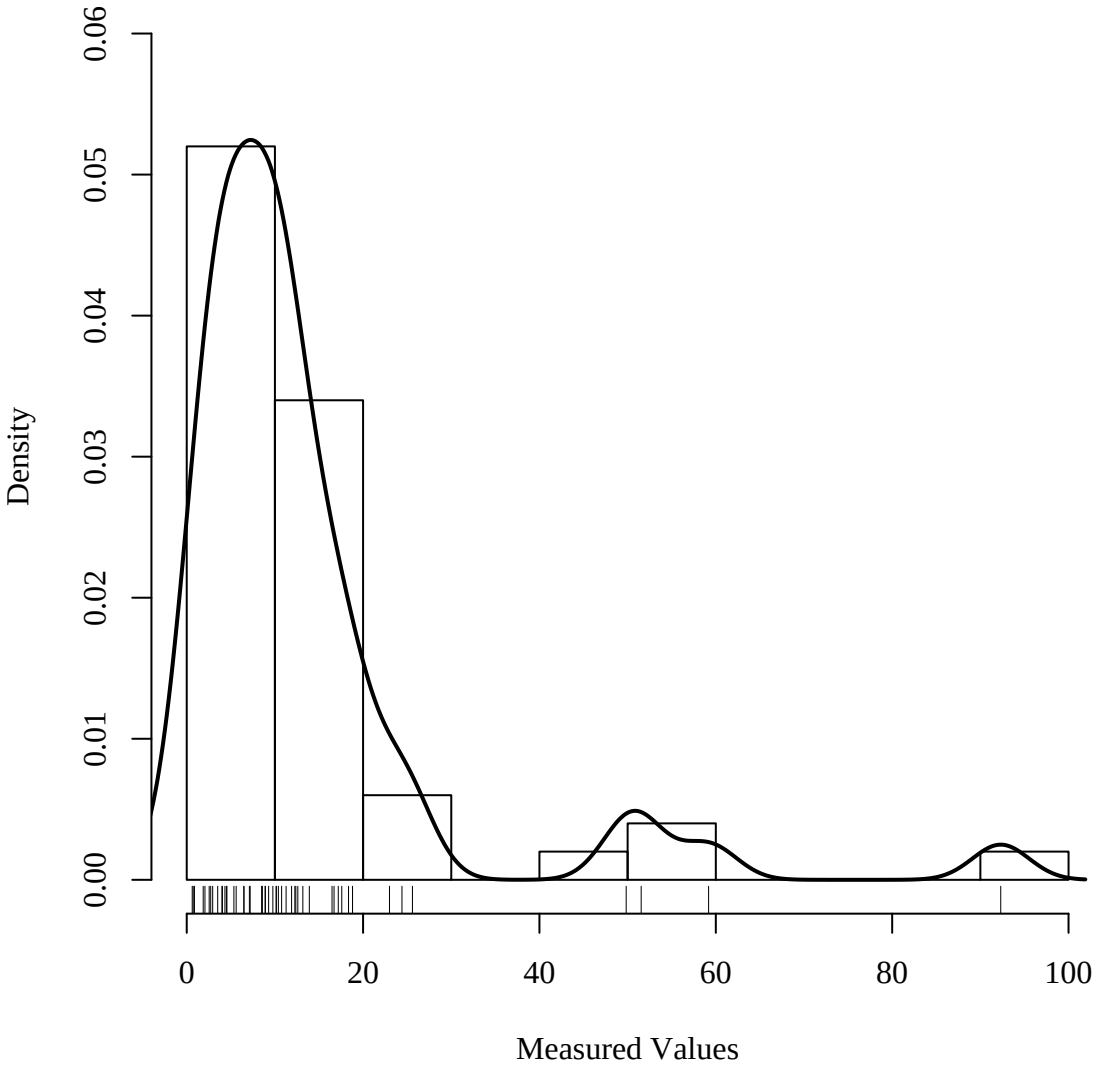

Figure 4.1. Example kernel density estimate. The data is a random sample of an input variable used in this thesis. The curve depicts the kernel density estimate. The short vertical lines between the histogram and the x-axis, called a rug, depict the data values.

Determining which parametric distribution best fits the uni-variate residual distribution requires the use of both the graphical and statistical tools. For each residual distribution, probable parametric distributions types were chosen for testing against the residual distribution. For each of these parametric distribution types, a best fit was generated using the maximum likely-hood estimator (MLE) method. These MLE results were then analyzed using Kolmogorov-Smirnov (K-S), Cramer-von Mises (CvM), and Anderson-Darling (A-D) goodness-of-fit tests to determine which distribution type best fit the uni-variate residual distribution. All three tests are non-parametric tests of continious uni-variate probability distributions. The K-S and CvM tests calculate the difference between the empirical cumulative density function (ECDF) of the test data and the cumulative density function (CDF) of the tested reference distribution. The K-S and CvM tests use different algorithms to perform the calculation. Each of the goodness-of-fit tests has their own strength and weaknesses and as such, graphical tools are used to confirm or refute the statistical test results (D'Agostino and Stephens 1986; Delignette-Muller and Dutang 2014; Venables and Ripley 2002).

4.4. River Storage Change

River reach estimated stored water volume changes ($\frac{\Delta S}{\Delta t}$) from equation 1 are the sum of the river segment stored water volume changes for each reach (Equation 9). The storage change for each segment is calculated independent of adjacent segments.

$$\frac{\Delta S}{\Delta t} = \sum \frac{\Delta S_i}{\Delta t} \tag{9}$$

Where:

$\Delta S =$ Water storage change in the river reach.

$\Delta S_i =$ Water storage change in river segment i.

$\Delta t =$ Model time step = 1 day.

River reach volume changes are calculated between two consecutive time steps. Reach volume changes are calculated as the sum of the volume changes within the segments that compose the reach. River segment volume change between time steps is calculated as shown in equation 10.

$$\frac{\Delta S_i}{\Delta t} = L_i \cdot \frac{\Delta A_i}{\Delta t} \tag{10}$$

Where:

$\frac{\Delta S_i}{\Delta t}$ = Segment storage change.

L_i = Segment length.

$\frac{\Delta A_i}{\Delta t}$ = Segment cross-section area change.

Figure 4.2 shows the difference between a simplified example of a natural channel and the modeled channel. Although the river is variable in width and depth along its entire lengths, it is modeled as a trapezoidal prism with a constant length and with a cross-section

that does not vary with respect to location. It was reasoned that this simplistic model would best approximate the average channel shape along the entire reach. The channel water surface elevation is assumed to be constant through each segment. This assumption is not true in nature, but we are not concerned with the water surface elevation, but with the flow depth. We are assuming that the flow depth remains relatively constant through a river segment. This assumes that all gains and losses to the river are accounted for either through flow gains and losses, evaporation, precipitation, or unaccounted for gains and losses as shown in equation 1.

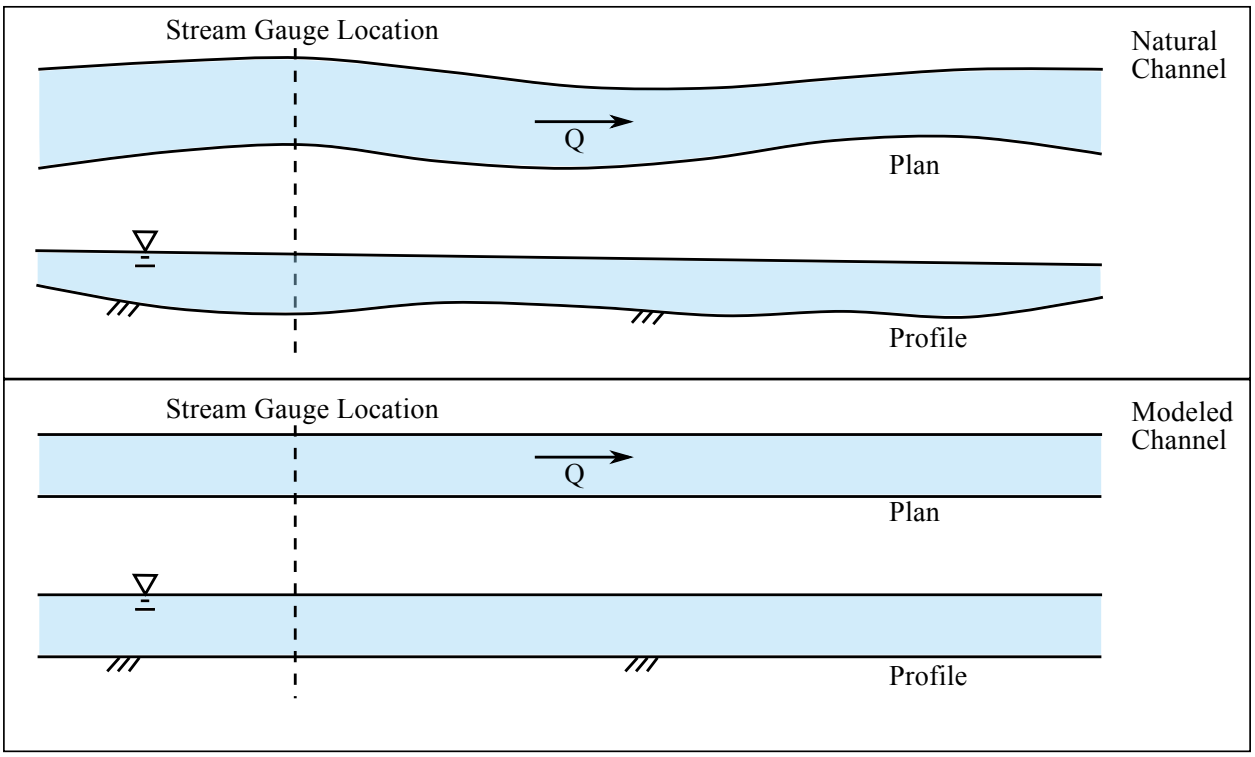

Figure 4.2. River Segment Model.

Segment lengths, as reported in Table 4.2, are sufficiently short such that any surges due to irrigation canal gates changes, precipitation events, or other events pass through the segment in less than a day. The total travel time is approximately 2-3 days and 1-2 days in the USR and DSR, respectively, based on USGS reported average stream velocity

measurements taken in conjunction with stream gauge calibrations. River segment length (L_i) was measured to the nearest 0.1 km using publicly available satellite imagery, USGS hydrography data, and geographical information system (GIS) software. River segment length was calculated as the length of the thalweg between the segment endpoints. When the USGS thalweg did not follow along the river channel as shown in the satellite imagery, a new thalweg was drawn. Rough validation of these measurements was performed in the field by comparing the GIS calculated length of adjacent roadways to the actual driven distance as reported by a vehicle odometer. River lengths are assumed to be constant throughout the study time frame. Individual and combined variations in the channel path along a river segment were assumed to be negligible.

Table 4.2. River Segment Lengths.

Study Reach	River Segment	Segment Length km	Segment Length mi
USR	A	12.5	7.8
	B	3.9	2.4
	C	30.7	19.1
	D	37.8	23.5
	E	14.3	8.9
DSR	F	37.6	23.4
	G	24.9	15.5

River segment cross-sectional area change $\left(\frac{\Delta A_i}{\Delta t}\right)$ calculation is based on the trapezoidal area that approximates the difference between the cross-sectional area at two different flow depths as depicted in Figures 4.3, 4.4 and in equation 11. While the cross sectional area difference isn't exactly a trapezoid, the difference for small differences in gauge height is insignificant.

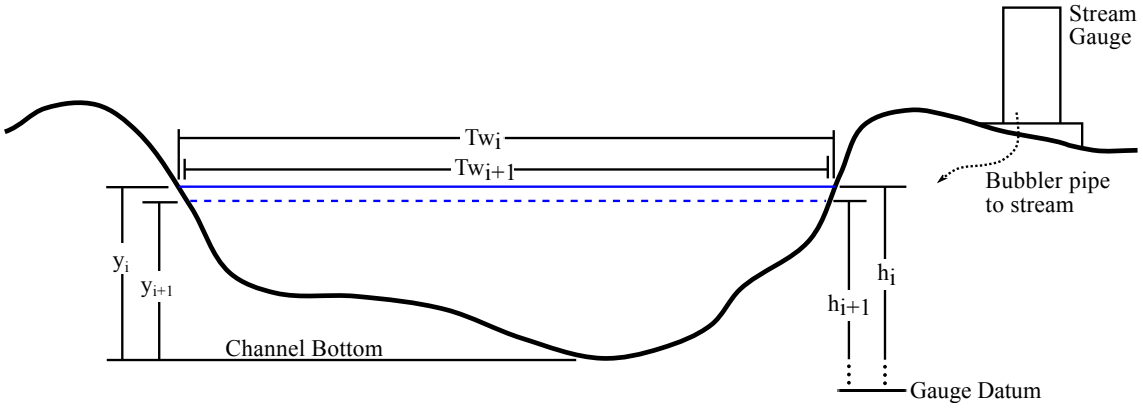

Figure 4.3. Average river segment cross-section area change.

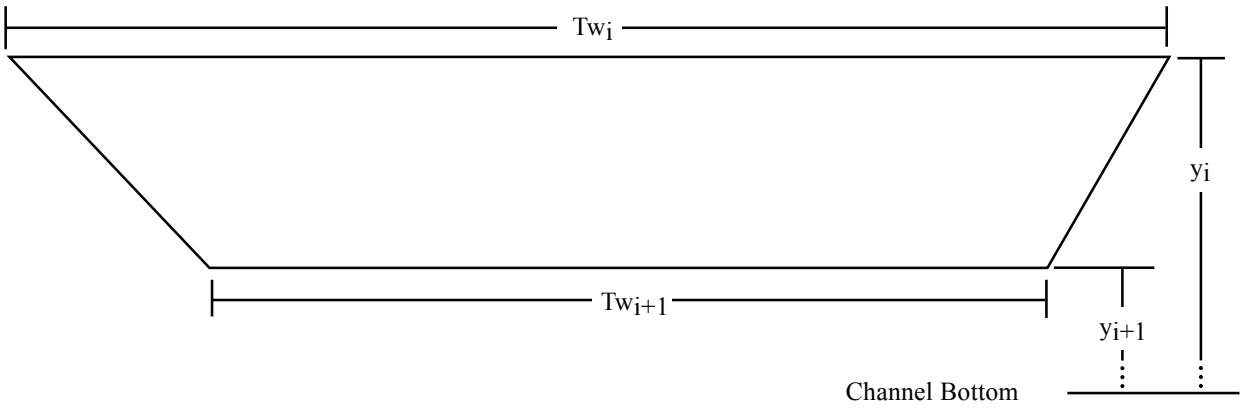

Figure 4.4. River cross-section area change diagram.

$$\begin{aligned}\frac{\Delta A_i}{\Delta t} &= \overline{Tw} \cdot \Delta y \\ \frac{\Delta A_i}{\Delta t} &= \frac{Tw_t + Tw_{t-1}}{2} \cdot (y_{t-1} - y_t) \end{aligned} \tag{11}$$

Where:

$_t$ = Current time step.

$_{t-1}$ = Previous time step.

$\frac{\Delta A_i}{\Delta t}$ = Cross-section area change at river section i between time steps.

$\overline{Tw}$ = Average river top width.

Δy = Change in flow depth from the previous time step.

Tw = River top width.

y = River flow depth.

Figure 4.3 shows a simplified river cross section at a stream gauge location. As previously discussed, stream gauges do not hold the channel bottom as their datum. They have an arbitrarily fixed datum that does not move unless reset by the gauge owner. The difference between the stream gauge datum and the channel bottom is corrected using a constant correction factor calculated from the river survey. The gauge datum does not have a known marker where the elevation could be directly measured. Instead, the surveyed water surface elevation was recorded at the gauge location on both sides of the channel. The flow depth value was calculated by finding the difference between the surveyed average water surface elevation and the surveyed channel bottom elevation. The flow depth was then compared to the stream gauge height reported for the same date and time as when the water surface elevation was surveyed. The difference between the reported value and the average of the surveyed values was taken as the correction factor for the gauge. This procedure was repeated for each gauge.

Flow depth values as reported by the USGS and CDWR are measured values with an associated probability range as calculated in equation 6. The uncertainties are applied

as shown in equation 12. A correction factor (C_i) is applied to each reported gauge depth to correct for the difference between the gauge datum and the channel bottom as measured during the channel cross-section survey. Two separate uncertainties are applied. ε_{h1} is the uncertainty distribution as described by the gauge owner. This uncertainty is reported by both the USGS and CDWR as being normally distributed with extreme values at ± 0.01 ft (± 0.003 m) (Cobb 1989). The second uncertainty term, ε_{h2}, is the result of personal observation of the river channel along its entire length. This term describes the variability in flow depth. It was observed that the channel depth did not vary greatly along most of its length. There were particular areas where there were deeper pools, but these areas were noted to be more prone to ponding during low flow. It is assumed that the average effective flow depth only varies within a normal distribution with limits of ± 0.076 m (± 0.25 ft). There is the possibility that ε_{h1} could cause the storage change between the time steps to change from a storage gain to a storage loss, or vise versa. This is acceptable as it is within the measurement limits of the instruments. Once $h + \varepsilon_{h1}$ has been calculated for the two successive time steps, the relationship between the two time steps is fixed. If the river segment flow depth rises between time steps after this calculation, then that relationship must continue throughout the rest of the volume change calculation. To facilitate this, it is assumed that ε_{h2} does not vary significantly within the study time frame and does not vary within a realization. The Arkansas River channel is sufficiently stable between consecutive days that this assumption is valid. A new ε_{h2} is drawn for each realization and remains constant for all time steps within the study time frame.

$$y_{i,t} = h_{i,t} + C_i + \varepsilon_{h1} + \varepsilon_{h2} \tag{12}$$

Where:

$y_{i,t}$ = Section i modeled average daily flow depth at time t.

$h_{i,t}$ = Section i reported average daily river gauge height at time t.

C_i = Section i river gauge height to flow depth correction term.

ε_{h1} = Reported river gauge height data uncertainty.

ε_{h2} = Estimated flow depth uncertainty.

Since the two uncertainty terms are both normal and additive to flow depth, they were added to produce a new normal distribution with mean equal to the sum of the means of the two distributions and standard deviation equal to the sum of the standard deviations of the two distributions. This additional step was taken to improve model calculation speed and to reduce the possible error of producing a total flow depth error that would cause a flow depth outside of the accepted range of 0.153 m to 1.53 m (0.5 ft to 5 ft). The uncertainty distributions ε_{h1} and ε_{h2} are not dependent on location, therefore all flow depth calculations draw from the same distribution. The normal distribution resulting from the addition of the ε_{h1} and ε_{h2} has a mean of zero and standard deviation of 0.007 07 m (0.020 32 ft) (Equation 13).

$$y_{i,t} = h_{i,t} + C_i + \mathcal{N}\left(\mu = 0m, \sigma = 0.00707m\right) \tag{13}$$

River top width (Tw) is calculated using equation 14. (Buhman, Gates, and Watson 2002; Gates and Al-Zahrani 1996). The river channel does not have a fixed cross-section along it's length, therefore, the fitting parameters, β_1 and β_2 are not constant, but are from distributions of β_1 and β_2. Equation 14 and the data from each survey cross-section was used to calculate a best fit equation using non-linear least squares regression. Regression results

justify

for each cross-section are presented in Table 4.3. There are an insufficient number of cross sections within each river segment to provide a statistically significant sample. This means that there is insufficient data available to generate independent fitting equations for each river segment. Therefore, the β_1 and β_2 values from each cross-section were combined to determine the distribution of β_1 and β_2 for the entire river reach. The combined distributions were tested to determine the best fit parametric distribution using the previously described method. The best fit distributions for β_1 and β_2 are presented in table 4.4. β_1 and β_2 values were analyzed for correlation which was found to be insignificant with a Pearson R value of 0.17. Visual analysis of the data points showed that there was no distinguishable pattern. Future cross-section surveys will expand the data set and may show that there is a correlation between β_1 and β_2, but the available data does not support that conclusion. Also presented in Table 4.4 is the best fit distribution for the residuals. These distributions and the distributions for β_1 and β_2 were analyzed to determine the best fit distribution using the methodology described in Section 4.3.

$$Tw_{i,t} = \beta_1 y_{i,t}^{\beta_2} + \varepsilon_{Tw} \tag{14}$$

Where:

$Tw_{i,t}$ = River segment i average daily top width at time step t.

$y_{i,t}$ = Calculated segment i average daily flow depth at time step t calculated using equation 12.

β_1 and β_2 = fitting parameter distributions.

ε_{Tw}= Calculated average daily flow depth uncertainty.

Table 4.3. Arkansas River segment top width estimating coefficients.

Study Region	River Segment	Cross-Section	Fitting Parameter β_1	Fitting Parameter β_2	Root Mean Squared Error
USR	A	1	219.1	0.5098	21.57
		2	197.5	0.01573	0.07938
		3	205.2	0.7734	32.05
		4	211.5	0.008948	0.2069
	B	5	59.4	0.9835	0.5002
		6	202	0.1382	12.48
		7	53.99	1.197	2.412
	C	10	141	0.5465	10.92
		11	187.2	0.5697	7.784
		12	277.9	0.01398	0.2358
		13	116.5	1.536	27.5
		14	110	0.917	1.986
	D	16	49.37	1.115	1.5171
		17	57.68	1.288	1.469
		18	116.4	0.5197	17.42
		19	58.35	0.3868	6.382
		21	141	0.07095	0.7172
		22	63.82	0.6103	1.132
		23	109.3	0.07456	0.4762
	E	26	47.62	0.1682	0.5901
DSR	F	1	22.48	0.4006	0.8139
		2	41.61	1.390	3.953
		3	29.82	0.2265	1.821
		4	21.46	0.3801	2.541
		5	22.78	0.8004	5.715
		6	26.21	0.4153	1.681
		7	41.92	1.487	3.299
	G	8	23.49	1.504	2.344
		9	33.54	1.106	3.676
		10	28.03	0.5790	2.003
		11	24.16	0.2103	1.693
		12	24.74	0.8992	2.617
		13	52.68	1.1850	5.757
		14	24.18	0.4764	0.9259

Non-linear regression models were used only when the specific model form, determined from known physical or geometrical relationships, was non-linear. R-squared values were not

used to determine goodness-of-fit for non-linear regression models since they can have valid R-squared values that are negative or greater than one (Spiess and Neumeyer 2010) and as such are outside of the boundary for comparing linear models. Pseudo or modified r-squared calculations are available, yet these computations result in values that are comparable to the r-squared value for linear models, but have slightly different interpretations . Since non-linear regression models were used only when specific model forms could be predetermined, there was no need to compare different model forms estimating the same result.

reference

Goodness-of-fit for non-linear regressions used in this thesis are purely for informational purposes. Since all non-linear models were based on known relationships, goodness-of-fit values only serve to show how well the data fits the model. In order to define non-linear regression model goodness-of-fit, the root mean squared error (RMSE) value was calculated. The RMSE represents the standard deviation of the differences between the predicted and observed values. The RMSE is scale dependent as the units are the same as the observed value. The RMSE is also known as the standard deviation. This would cause an issue if models for different observed value units and scales were compared against each other. In this study, non-linear regression models are only used to estimate the cross-sectional width of a river segment and to estimate the selenium concentration at one location. Since all cross-section analyses use the same measurement units, this allows us to compare the residual errors associated with the various cross sections without needing to consider scale or units.

The results of the top width equation for each cross-section, generated through non-linear regression, was compared to the observed results to visually compare the goodness-of-fit for each cross-section. Figure 4.5 is an example

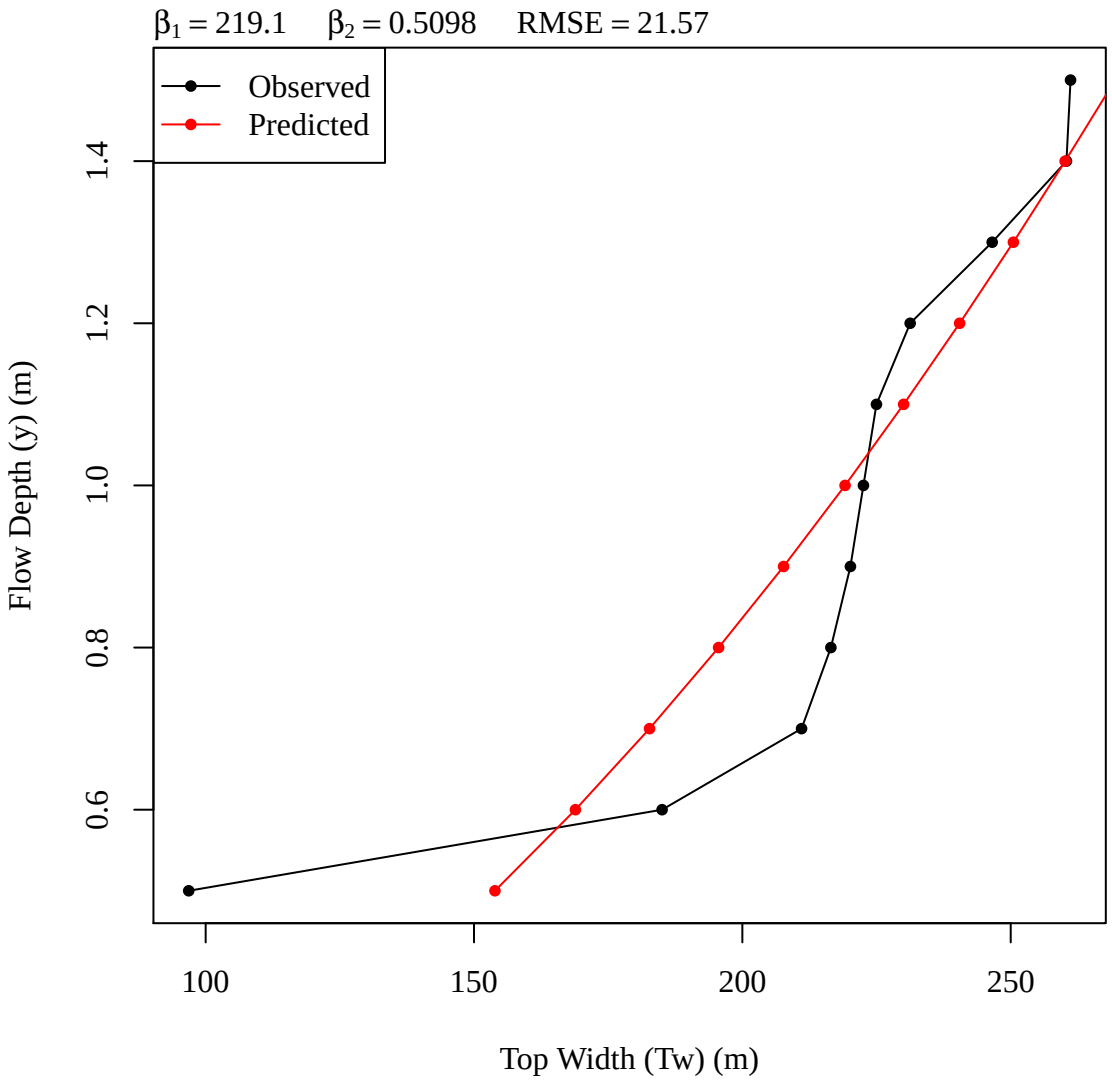

Figure 4.5. Example Flow Depth vs. River Top Width Relationship. The non-linear best fit line of the form in Equation 14 is red. The values are the two non-linear regression fitting parameters (β_1 and β_2) and the residual standard error for the fitting equation (σ). Similar figures for all cross-sections are found in the appendix.

Values β_1 and β_2 are drawn from probability distributions. Calculated flow depth and river top width data pairs were used to determine the distributions from which β_1 and β_2 in equation 14 were drawn. These distributions were developed using non-linear, least-squares regression. Values below 0.15 m (0.5 ft) were removed from the regression analysis. Flow values below this depth are not common and it was determined that these points would not

Table 4.4. River top width fitting parameter distributions.

Study Reach	Fitting Parameter	Best Fit Distribution		
		Dist. Shape	p1*	p2*
USR	β_1	logistic	16.8	7.53
	β_2	log-normal	-1.27	1.57
	Residual	logistic	1.99	0.99
DSR	β_1	logistic	28.2	4.84
	β_2	log-normal	-0.43	0.65
	Residual	log-normal	0.87	0.57

* Distribution fitting parameters. For logistic, p1=location and p2=scale. For log-normal, p1=mean of the log scale and p2=standard dev. of the log scale

allow for an accurate representation of the flow depth to river top width relationship for the range of known flow depths. Values above 1.52 m (5.0 ft) were also removed from the regression analysis. Flow depths above this depth are above the banks of the primary river channel and are within the inner flood plain. Table 4.3 gives the resulting β_1 and β_2 values for each surveyed cross-section. Figure 4.5 is an example of the surveyed flow depth and river top width relationships and the derived non-linear relationship for cross-section 1 in river segment A of the USR. Similar relationship plots for the other surveyed cross-sections are found in the appendix.

Figure 4.6 shows the distributions of β_1 and β_2 values and the various best-fit distributions in both the USR and DSR. Logistic, normal, exponential, Weibull, and log-normal distributions were fitted to the data. Vertical tick marks in the x-axis margin are at the data values. Kernel density estimations were used as an alternative means to graphically represent the data density.

The resulting river shape parameter distributions are valid for the river reach for which they were calculated. Each river segment draws values from the shape parameter distributions independently. Only one pair of shape parameters is drawn for each realization.

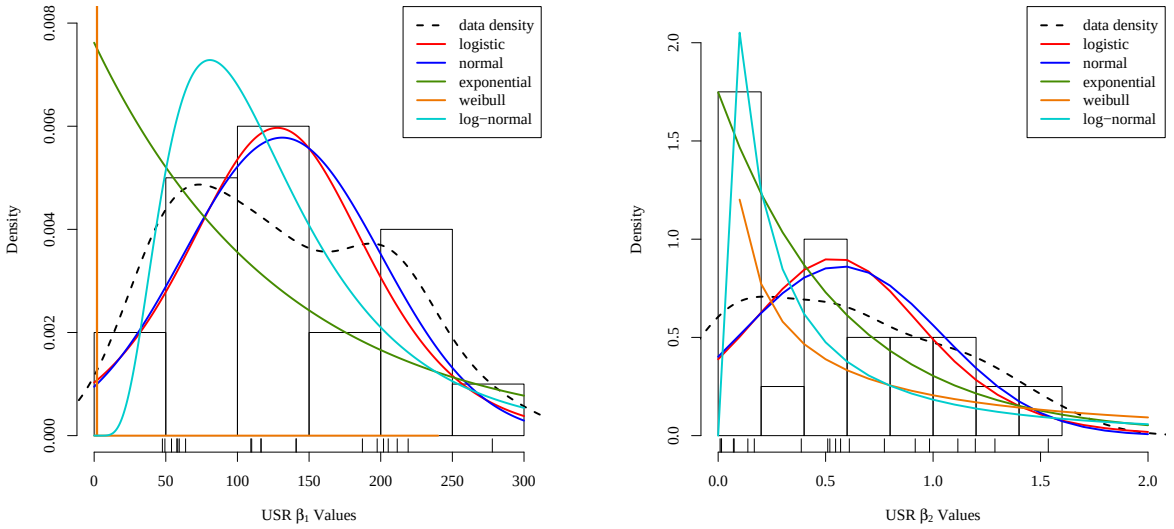

(a) USR β_1 **(b)** USR β_2

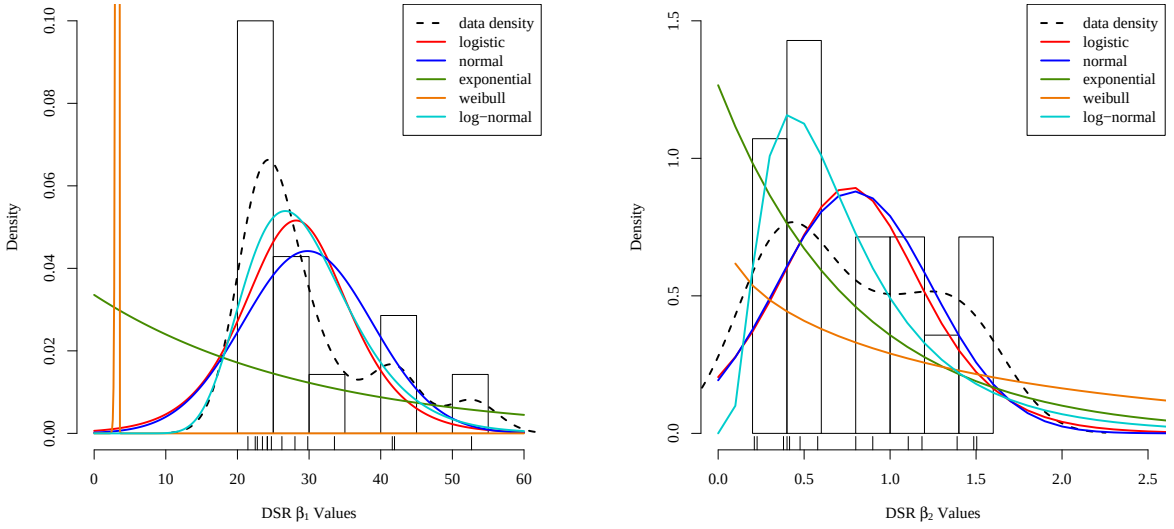

(c) DSR β_1 **(d)** DSR β_2

Figure 4.6. *Tw* Versus *h* Fitting Parameter β_1 and β_2 Distributions. The black dashed line is a kernel density plot representing a histogram where the bin size approaches zero. The colored curves are the best fit for the particular distribution type. Vertical tick marks in the x-axis are at the data values.

It is assumed that the river geometry does not significantly change within the study time frame. Channel variability is modeled between the realizations.

Residuals from the non-linear regression analyses were combined into a single data set for uncertainty analysis. Combining this data set was a logical step following the combination

of the data that generated the residuals. Residuals were tested using the same tools and techniques used to test the river shape parameter distributions. USR and DSR channel shape residuals were found to have a log-normal distribution. Figure 4.7 presents the residuals distribution analyses for the USR and DSR. These figures are of the same type as those used to analyze the river shape parameter distributions, figure 4.6.

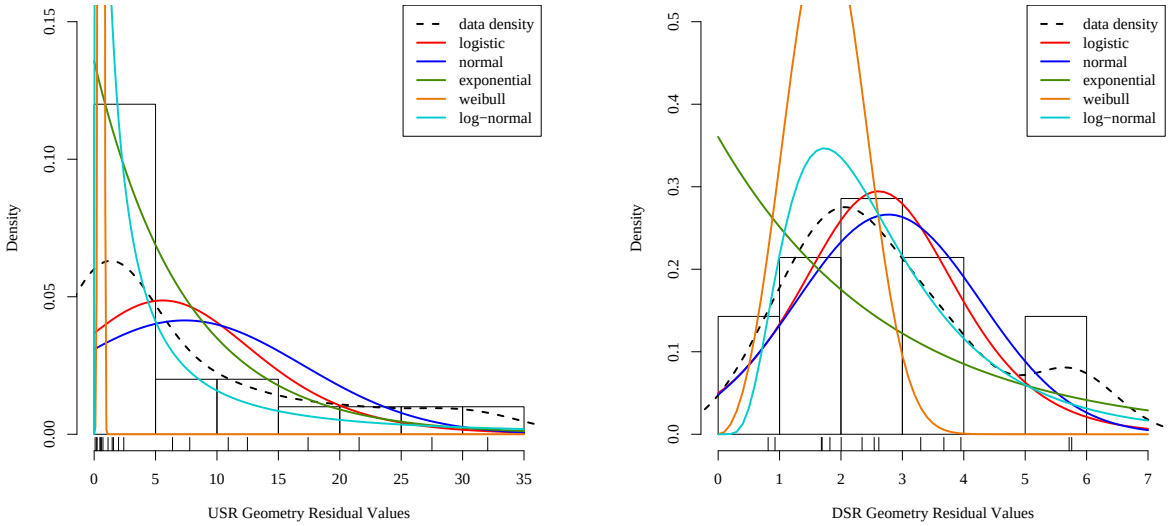

(a) USR Residuals **(b)** DSR Residuals

Figure 4.7. Tw versus H Residuals Distribution. The black dashed line is a kernel density plot representing a histogram where the bin size approaches zero. The colored curves are the best fit for the particular distribution type. Vertical tick marks in the x-axis are at the data values.

Residuals are the collection of the difference between the calculated regression model values and the measured values. Collectively, the distribution of the residuals describe the uncertainty of the regression model. In this case, the distribution of residuals describe the top width estimating uncertainty ε_{Tw}. Residuals should be tested for heteroskedasticity to determine if the model does not adequately predict the data. Heteroskedasticity is the condition where the variability of a variable, in this case the residuals, is unequal across the range of the values and is usually indicative of under specification of the model. There are

many tests for heteroskedasticity, but the most powerful is visual analysis of the plot of the residuals against the fitted, or calculated, values. When a small number of values is used to perform the regression, visual and computational analysis becomes difficult since patterns may appear that don't truly exist or patterns may not appear where they do exist. When heteroskedasticity was evident during model creation, the model was modified to remove the heteroskedasticity. Other methods are available to account for heteroskedasticity, but the most strongly recommended is model modification. Determining the parametric distribution that best fits the regressions is performed using the method described in section 4.3. Both visual and goodness-of-fit tests were applied to all residual regression analyses.

Results from the individual regression and residuals analyses are plotted with the source data to visually determine if the resulting best fit estimating equation or residuals distribution suitably fit the source data. An example of one of these figures is Figure 4.5 which plots a best fit regression equation alongside the source data. Figure 4.7 is representative of how the residual analysis results are visually analyzed. The best fit of several different distribution shapes are plotted over the histogram and KDE of the residuals or source data. These types of figures are used throughout the analysis to visually verify that the calculated regression models and best-fit distributions actually fit the data.

Results from deterministic and stochastic models are presented throughout this thesis. While both model types present results from the same source data, stochastic models, as previously discussed, also include uncertainty in many forms. Stochastic model results are complex. They are time-series models where each time step is an independent distribution of the results. Figure is a very simple representation of a time-series. The top sub-figure shows a sine curve which represents the deterministic model. The second sub-figure shows one realization of the stochastic model which is the deterministic model with uncertainty

added at each time step. For this example, the uncertainty is normally distributed within the time step. The third sub-figure is 500 independent realizations shown on top of each other. The fourth sub-figure shows the 500 realizations with three calculated lines representing stochastic model summary statistics time-series.

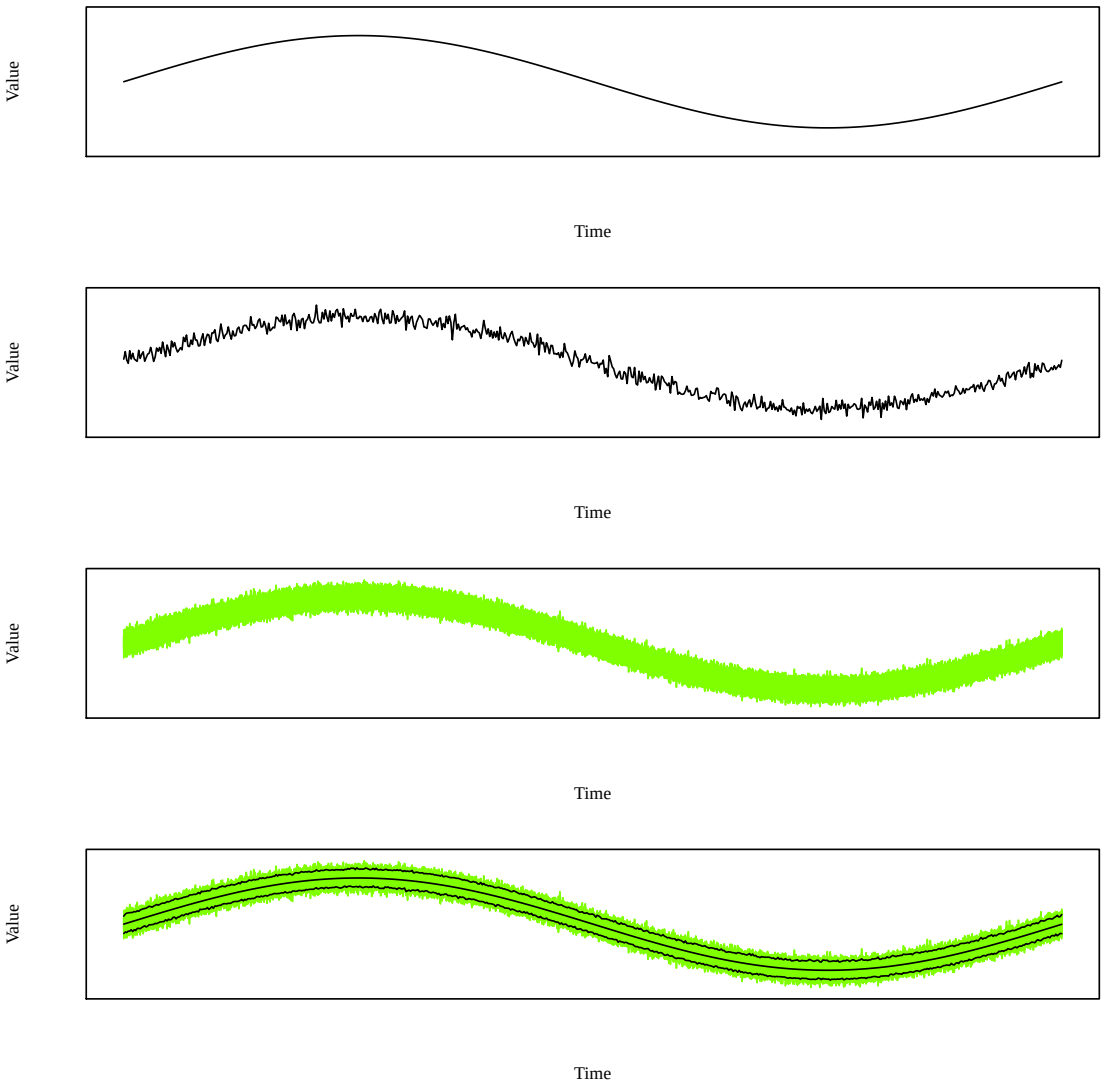

Figure 4.8. Stochastic model graphical results presentation description. The top sub-figure represents a simple deterministic time-series model. The second sub-figure represents a single stochastic time-series model. The third sub-figure represents 500 stochastic time-series. The fourth sub-figure shows the 500 stochastic time-series with the three stochastic model summary statistics time-series. The top line is the 97.5th percentile time-series, the middle line is the mean time-series, and the bottom line is the 2.5th percentile time-series.

The middle line is the time-series that represents the mean value calculated for each time-step. This is the stochastic model mean time-series. The top and bottom lines are the 97.5th and 2.5th percentile calculated for each time step. These are the stochastic model 97.5th percentile time-series and stochastic model 2.5th percentile time-series, respectively. Collectively, these three time-series are called stochastic model summary statistics time-series. These three time-series show how the results and range of possible results vary with time. All stochastic time-series graphs present only the three stochastic model summary statistics time-series. Values outside of these are not plotted so as to improve understanding and readability of the graphical results

Presenting individual values for stochastic model results requires further summary statistics of the calculated stochastic model summary statistics time-series. Without this further reduction, results would contain large quantities of values which are very difficult to present. The mean, 97.5th percentile, and 2.5th percentile are calculated for each of the summary statistics time-series to provide more readable results. The summary statistics for each of the stochastic model summary statistics time-series indicate the most likely value and the range of possible values as presented in the example in Table 4.5. In this table, each row of the bottom portion of the table presents one of the stochastic model summary statistic time-series results. In this example, values 'g', 'h', and 'i' are the summary statistics for the stochastic model mean time-series.

Table 4.5 also includes the deterministic time-series summary statistics values. These values are the 2.5th percentile, mean, and 97.5th percentile calculated from the deterministic model results and are presented in the upper half of the table. The deterministic model time-series summary statistics should be approximately the same as the stochastic model mean time-series summary statistics, which are values g, h, and i in the lower half of the

table. This statement should be true if the deterministic model is a possible realization of the stochastic model and if the distribution of the combined uncertainties in the stochastic model are approximately normally distributed.

Table 4.5. Example deterministic and stochastic model numerical results. The single row on on the deterministic model side presents the summary statistics for the deterministic model (values a, b, and c). Each row on the stochastic model side presents the results for a specific stochastic model summary time-series. All values are presented in common units. The Pearson Correlation value (m) is calculated between the deterministic model time-series and the stochastic model mean time-series values at each time-step in the models.

Deterministic Model Time Series			
	2.5th Percentile	Mean	97.5th Percentile
	a	b	c
Stochastic Model Summary Statistics Time Series			
	2.5th Percentile	Mean	97.5th Percentile
97.5th Percentile	d	e	f
Mean	g	h	i
2.5th Percentile	j	k	l
Pearson Correlation = m			

One goal of stochastic modeling is to have a deterministic model that resides within the stochastic. If the deterministic model isnt a possible realization of the stochastic model, then there are significant stochastic model issues that need to be addressed. Ideally, the stochastic model mean time-series at each time step should be close to the deterministic model at that same time step. To determine if this relationship is true, the Pearson correlation between the stochastic model mean time-series and the deterministic model was calculated and is included at the bottom of Table 4.5. Calculating the Pearson correlation requires assuming the two compared data sets are continuous and are linearly related. All input values and results in this thesis are continuous, either from zero to $+\inf$ or between $\pm\inf$.

Correlation values only provides a numerical value to describe the relationship between two values or data sets. It does not imply causality or linearity. We can infer causality because the deterministic model is a subset of the stochastic model. In fact, the deterministic model was used to create the stochastic model. We cannot infer linearity. Figure attempts to answer the linearity issue through visual analysis. The black dots are the comparison of the stochastic mean time-series and the deterministic model. The red and blue does are the comparison of the stochastic 97.5th and 2.5th percentile time-series as compared to the deterministic model, respectively. The solid black line follows the equation y=x. This is where all of the black dots should lie if the stochastic mean time-series and deterministic models were in perfect agreement. The dashed line is the quadratic best fit line through the stochastic mean time-series.

River segment B in the USR does not have a flow gauge within its boundaries and therefore has no reported flow depths. This segment has an additional irrigation diversion check structure within its boundaries, thereby sub-dividing segment B into two sub-segments, each with its own ungauged flow depth. Due to segment B being the shortest, composing only 3.9% of the USR's total length, and the additional variability of the possible flow depth, the average daily flow depth within segment B is taken as the mean of the reported flow depths in segment A and C. Top width and volume change calculation follows the previously described methodology.

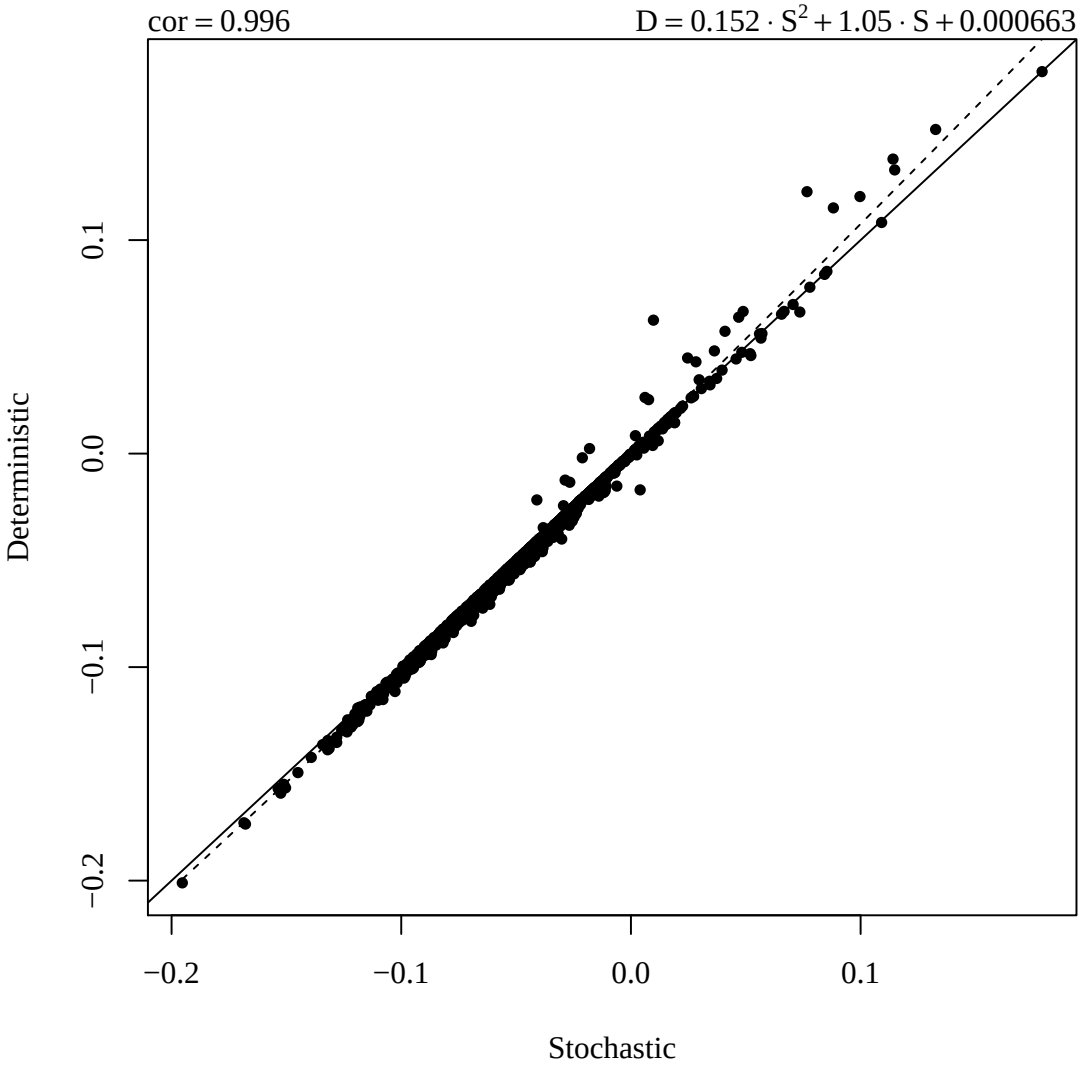

Figure 4.9. Example scatterplot comparing deterministic model time-series and stochastic model mean time-series results. The solid line is drawn such that $y = x$. The dashed line is the best-fit quadratic equation between the deterministic model time-series and the stochastic model mean time-series and the equation is in the top right. The Pearson Correlation is the top left number.

4.4.1. *River Storage Change Results*

The time-series plots of all four stochastic geometric parameters for each study region river section segment is presented in Figures 4.10 and 4.11 for the USR and DSR, respectively. The black lines indicate the stochastic model mean time-series. The blue band indicates the 95% central inter-percentile range (CIR) of the stochastic values as defined by the stochastic model 2.5th percentile time-series and the stochastic model 97.5th percentile time-series. The red dashed line in the flow depth portion of the figure indicates the reported flow depth values. It is plotted under the stochastic model mean time-series line and as such is only visible when either the stochastic model mean time-series value was not calculated due to missing data or when the two values deviate.

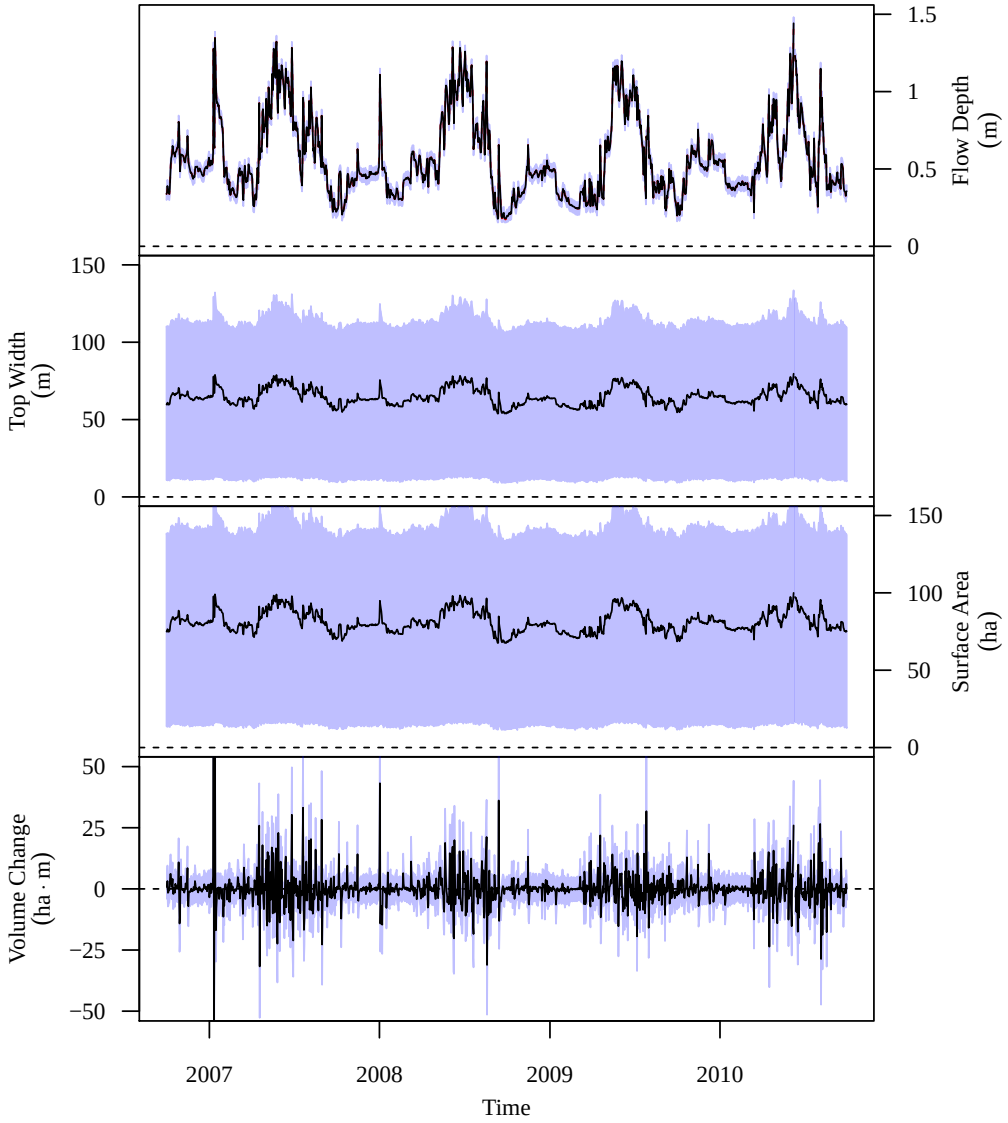

(a) Segment A

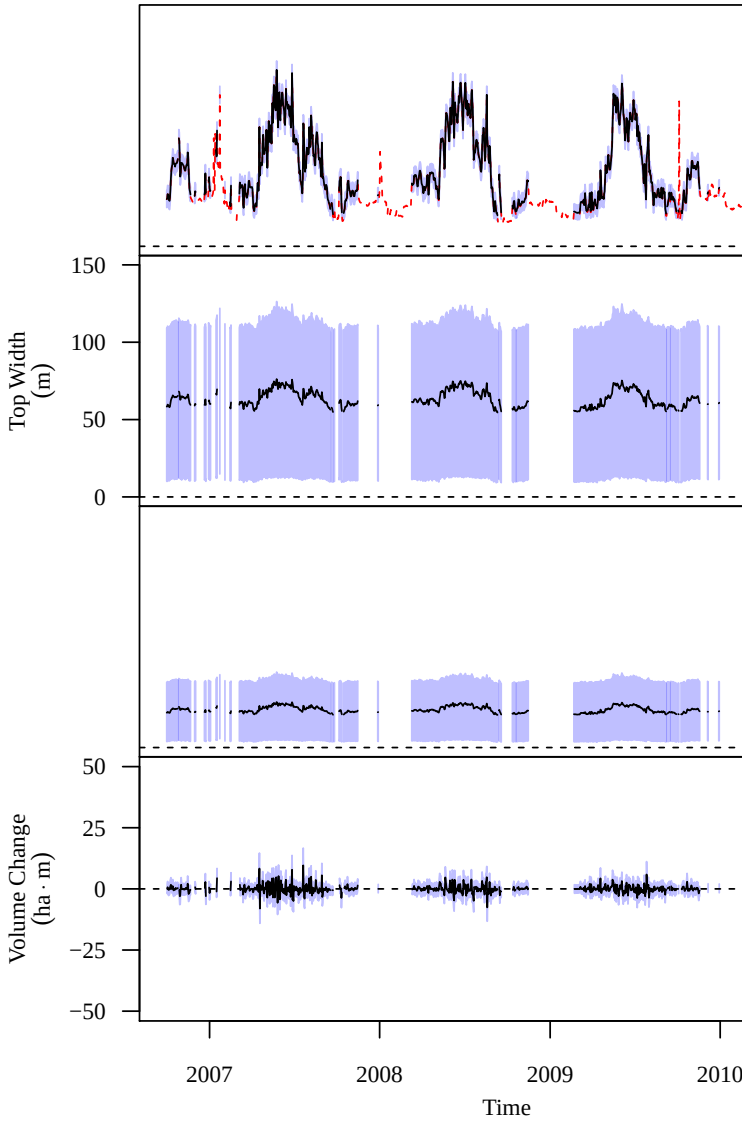

(b) Segment B

Figure 4.10. USR stochastic geometric parameter time-series. The black lines indicate the stochastic model mean time-series. The blue band indicates the 95% central inter-percentile range (CIR) of the stochastic values. The red dashed line in the flow depth portion of the figure indicates the reported flow depth values.

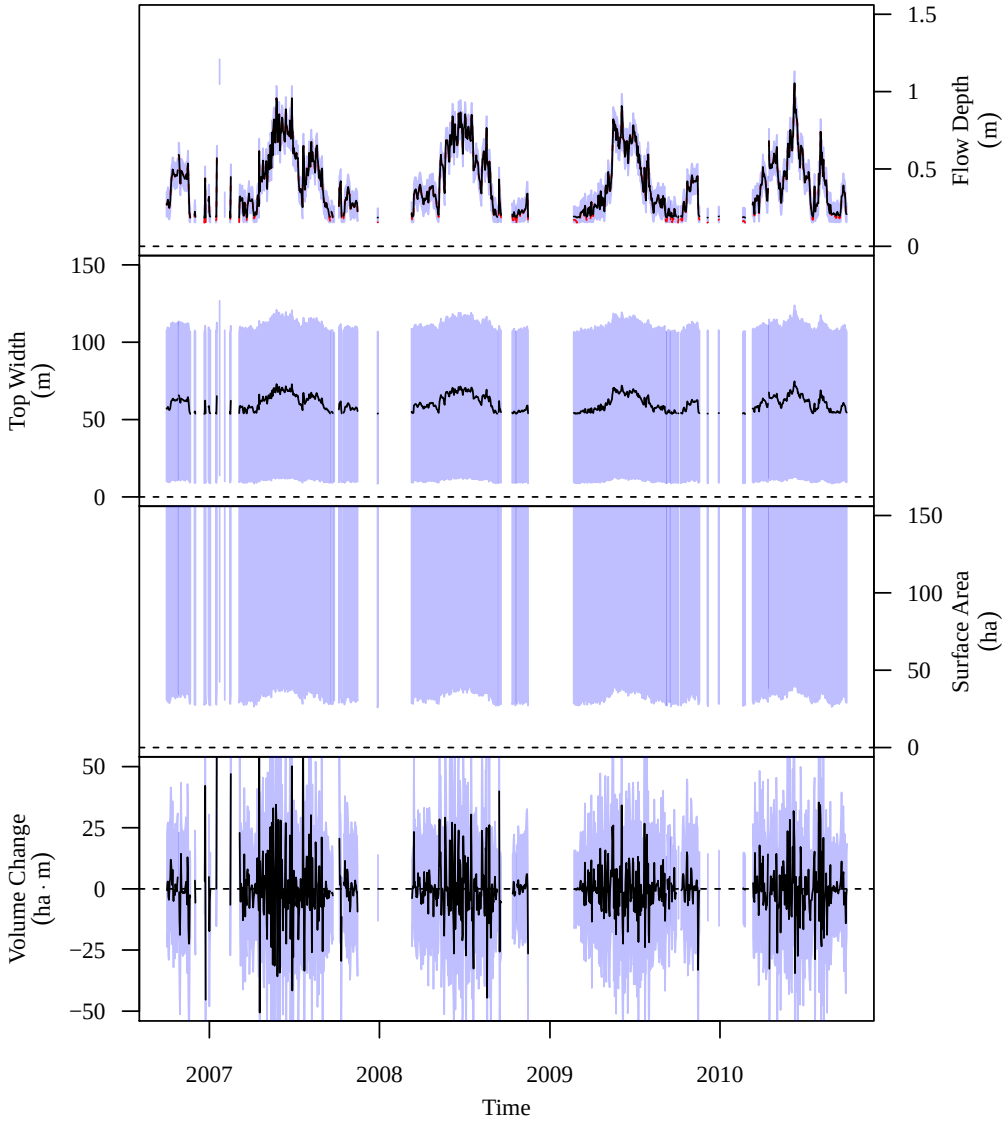

(a) Segment C

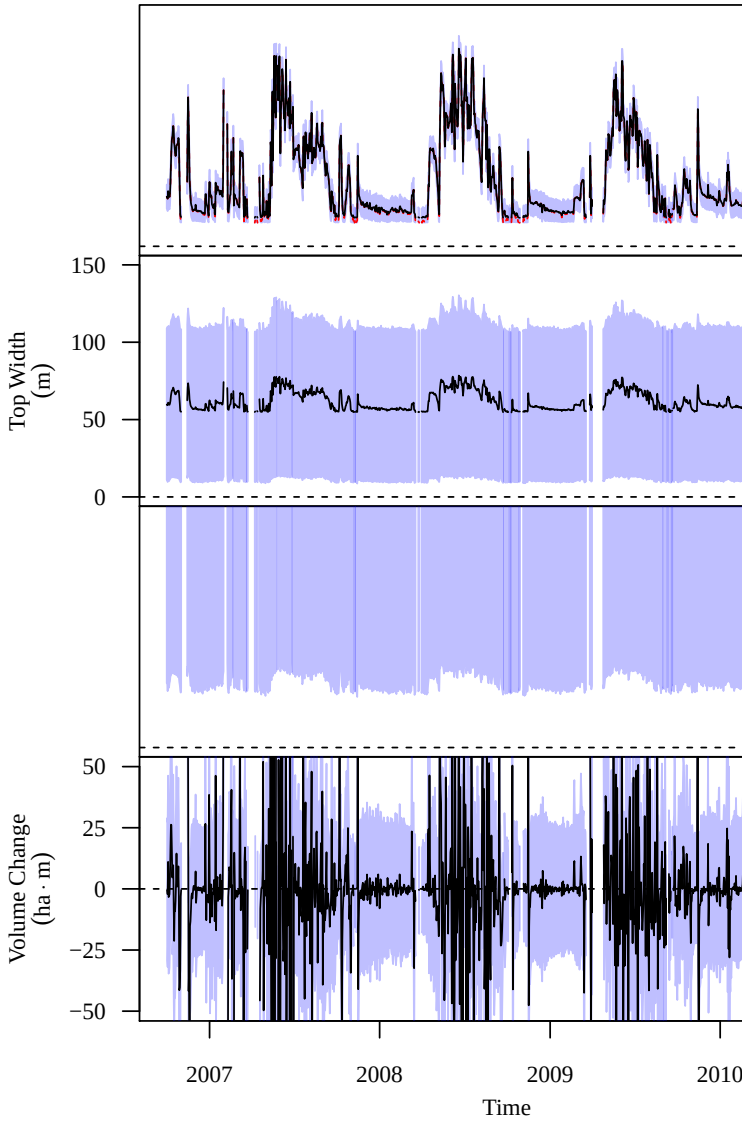

(b) Segment D

Figure 4.10 (Cont). Stochastic geometric parameter time-series.

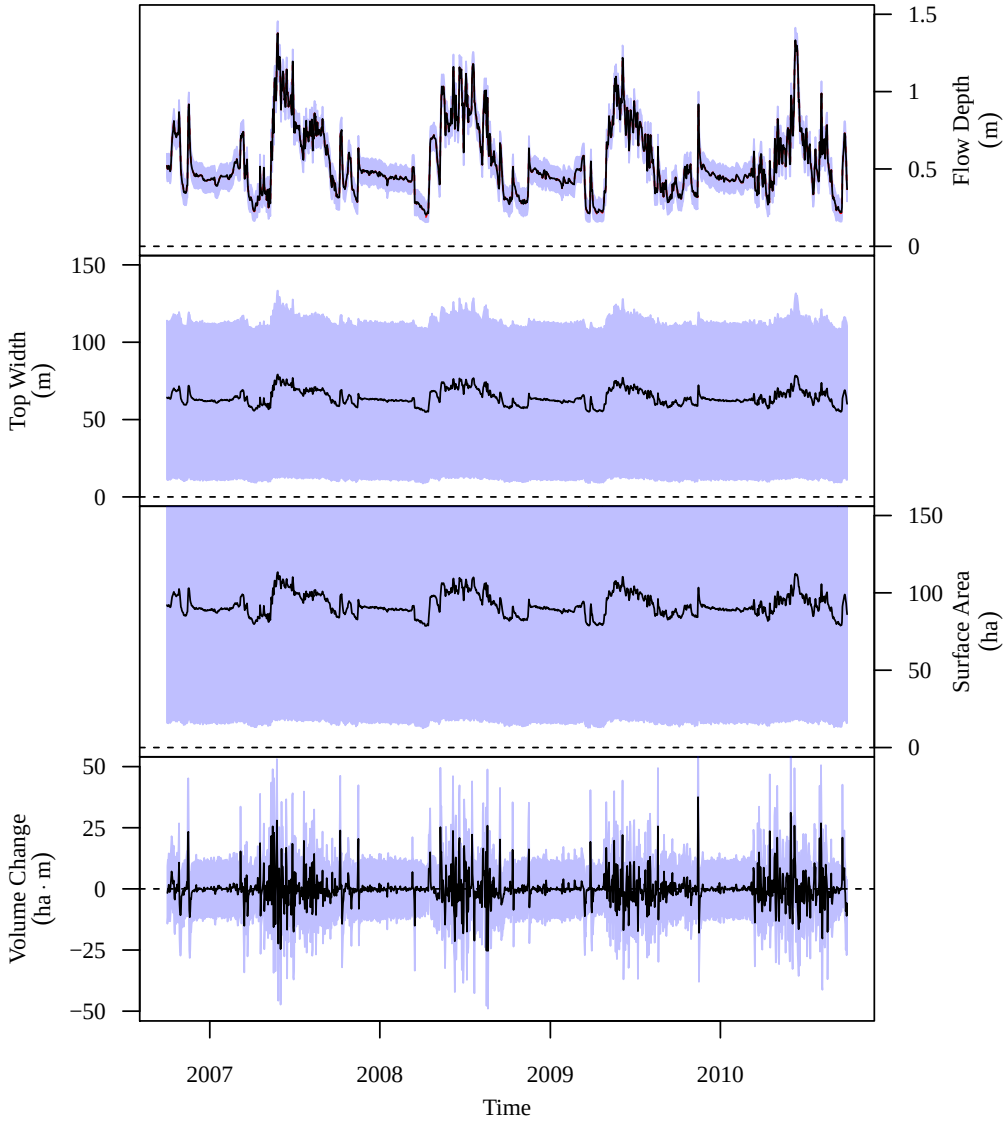

(a) Segment E

Figure 4.10 (Cont). Stochastic geometric parameter time-series.

Figure 4.11. DSR stochastic geometric parameter time-series. The black lines indicate the stochastic model mean time-series. The blue band indicates the 95% central inter-percentile range (CIR) of the stochastic values. The red dashed line in the flow depth portion of the figure indicates the reported flow depth values.

Table 4.6. USR river segment A surface area deterministic and stochastic model numerical results. Values are in hectares (acres).

Deterministic Model Time Series			
	2.5th Percentile	Mean	97.5th Percentile
	106.2 (262.4)	134.3 (331.9)	167.1 (412.9)
Stochastic Model Summary Statistics Time Series			
	2.5th Percentile	Mean	97.5th Percentile
97.5th Percentile	134.6 (332.6)	142.7 (352.6)	158.4 (391.4)
Mean	70.1 (173.2)	81.43 (201.2)	95.74 (236.6)
2.5th Percentile	12.05 (29.78)	14.8 (36.57)	17.52 (43.29)

Pearson Correlation = 0.9985

Table 4.7. USR river segment B surface area deterministic and stochastic model numerical results.

Deterministic Model Time Series			
	2.5th Percentile	Mean	97.5th Percentile
	30.55 (75.49)	38.51 (95.16)	48.96 (121)
Stochastic Model Summary Statistics Time Series			
	2.5th Percentile	Mean	97.5th Percentile
97.5th Percentile	41.49 (102.5)	43.66 (107.9)	47.02 (116.2)
Mean	21.49 (53.1)	24.65 (60.91)	28.48 (70.38)
2.5th Percentile	3.739 (9.239)	4.548 (11.24)	5.408 (13.36)

Pearson Correlation = 0.9982

Figures 4.10 and 4.11 were analyzed to verify that direct correlations existed between the flow depth and the calculated geometric parameters. Top width and surface area should increase and decrease in proportion with the increase and decrease in flow depth. Volume changes are based on two flow depth values and do not have a direct correlation to the flow depth displayed in the figure. All of the river sections show the correct correlations between flow depth and the calculated river geometric parameters.

Table 4.8. USR river segment C surface area deterministic and stochastic model numerical results.

Deterministic Model Time Series			
	2.5th Percentile	Mean	97.5th Percentile
	237.2 (586.1)	300.9 (743.5)	372.1 (919.5)
Stochastic Model Summary Statistics Time Series			
	2.5th Percentile	Mean	97.5th Percentile
97.5th Percentile	326 (805.6)	341.2 (843.1)	363.2 (897.5)
Mean	165.9 (409.9)	187.4 (463.1)	216.8 (535.7)
2.5th Percentile	27.49 (67.93)	33.26 (82.19)	39.83 (98.42)

Pearson Correlation = 0.9959

Table 4.9. USR river segment D surface area deterministic and stochastic model numerical results.

Deterministic Model Time Series			
	2.5th Percentile	Mean	97.5th Percentile
	290.3 (717.3)	373.7 (923.4)	497.8 (1230)
Stochastic Model Summary Statistics Time Series			
	2.5th Percentile	Mean	97.5th Percentile
97.5th Percentile	403.9 (998.1)	424.2 (1048)	470.9 (1164)
Mean	208.3 (514.7)	235.7 (582.4)	286.5 (708)
2.5th Percentile	35.28 (87.18)	43.12 (106.6)	54.18 (133.9)

Pearson Correlation = 0.9968

Table 4.10. USR river segment E surface area deterministic and stochastic model numerical results.

Deterministic Model Time Series			
	2.5th Percentile	Mean	97.5th Percentile
	121.1 (299.2)	152 (375.6)	187.5 (463.3)
Stochastic Model Summary Statistics Time Series			
	2.5th Percentile	Mean	97.5th Percentile
97.5th Percentile	155.1 (383.3)	162.8 (402.3)	178 (439.8)
Mean	80.04 (197.8)	92.11 (227.6)	107.7 (266.1)
2.5th Percentile	13.69 (33.83)	16.75 (41.39)	19.62 (48.48)

Pearson Correlation = 0.9983

Table 4.11. USGS Measured Field Parameter Accuracy Rating Table. This table was taken from the USGS annual water data report.

Measured field parameter	**Ratings of accuracy (Based on combined fouling and calibration drift corrections applied to the record)**			
	Excellent	**Good**	**Fair**	**Poor**
Water temperature	≤ ± 0.2 °C	> ± 0.2 - 0.5 °C	> ± 0.5 - 0.8 °C	> ± 0.8 °C
Specific conductance	≤ ± 3%	> ± 3 - 10%	> ± 10 - 15%	> ± 15%
Dissolved oxygen	≤ ± 0.3 mg/L or ≤ ± 5%, whichever is greater	> ± 0.3 - 0.5 mg/L or > ± 5 - 10%, whichever is greater	> ± 0.5 - 0.8 mg/L or > ± 10 - 15%, whichever is greater	> ± 0.8 mg/L or > ± 15%, whichever is greater
pH	≤ ± 0.2 units	> ± 0.2 - 0.5 units	> ± 0.5 - 0.8 units	> ± 0.8 units
Turbidity	≤ ± 0.5 turbidity units or ≤ ± 5%, whichever is greater	> ± 0.5 - 1.0 turbidity units or > ± 5 - 10%, whichever is greater	> ± 1.0 - 1.5 turbidity units or > ± 10 - 15%, whichever is greater	> ± 1.5 turbidity units or > ± 15%, whichever is greater

References

Buhman, Daniel L., Timmothy K. Gates, and Chester C. Watson (2002). "Stochastic Variability of Fluvial Hydraulic Geometry: Mississippi and Red Rivers." In: *Journal of Hydraulic Engineering* 128.4, pp. 426–437.

Cobb, Ernest D. (1989). *Programs and Plans–Policy Statement on Stage Accuracy.* USGS. URL: `http://water.usgs.gov/admin/memo/SW/sw89.08.html`.

D'Agostino, Ralph B. and Michael A. Stephens, eds. (1986). *Goodness-of-fit-techniques (Statistics: a Series of Textbooks and Monographs, Vol. 68)*. 1st ed. Dekker. ISBN: 9780824774875.

Delignette-Muller, Marie Laure and Christophe Dutang (2014). "fitdistrplus: An R Package for Fitting Distributions." In:

Gates, Timmothy K. and Muhammad A. Al-Zahrani (1996). "Spatiotemporal Stochastic Open-Channel Flow. I: Model And Its Parameter Data." In: *Journal of Hydraulic Engineering* 122.11, pp. 641–651.

Haan, C. T. (1989). "Parametric Uncertainty in Hydrologic Modeling." In: *Transactions of the ASAE* 32.1, pp. 0137–0146.

Haan, Charles Thomas (2002). "Statistical methods in hydrology." In:

Harmel, R Daren and Patricia K Smith (2007). "Consideration of measurement uncertainty in the evaluation of goodness-of-fit in hydrologic and water quality modeling." In: *Journal of Hydrology* 337.3, pp. 326–336.

Herschy, RW (2002). "The uncertainty in a current meter measurement." In: *Flow Measurement and Instrumentation* 13.5, pp. 281–284.

ISO (2008). "Guide to the Expression of Uncertainty in Measurement, (1995), with Supplement 1, Evaluation of measurement data, JCGM 101: 2008." In: *Organization for Standardization, Geneva, Switzerland*.

Spiess, Andrej-Nikolai and Natalie Neumeyer (2010). "An evaluation of R2 as an inadequate measure for nonlinear models in pharmacological and biochemical research: a Monte Carlo approach." In: *BMC pharmacology* 10.1, p. 6.

Venables, William N and Brian D Ripley (2002). *Modern applied statistics with S*. Springer Science & Business Media.

Vicens, Guillermo J., Ignacio Rodríguez-Iturbe, and John C Schaake (1975). "Bayesian generation of synthetic streamflows." In: *Water Resources Research* 11.6, pp. 827–838.

Wanielista, Martin, Robert Kersten, Ron Eaglin, et al. (1997). *Hydrology: Water quantity and quality control*. John Wiley and Sons.